01 Jul 2000

Direct Measurement of Oscillations between Degenerate Two-Electron Bound-State Configurations in a Rapidly Autoionizing System

Heider N. Ereifej

J. Greg Story
Missouri University of Science and Technology, story@mst.edu

Recommended Citation

H. N. Ereifej and J. G. Story, "Direct Measurement of Oscillations between Degenerate Two-Electron Bound-State Configurations in a Rapidly Autoionizing System," *Physical Review A - Atomic, Molecular, and Optical Physics*, vol. 62, no. 2, pp. 023404-1-023404-5, American Physical Society (APS), Jul 2000.
The definitive version is available at https://doi.org/10.1103/PhysRevA.62.023404

Direct measurement of oscillations between degenerate two-electron bound-state configurations in a rapidly autoionizing system

Heider N. Ereifej and J. G. Story
Department of Physics, University of Missouri–Rolla, Rolla, Missouri 65409-0640
(Received 15 February 2000; published 18 July 2000)

In this paper we report a direct observation of the oscillation between bound-state configurations in a rapidly autoionizing system. Calcium atoms were excited to a pure $4p_{3/2}nd$ two-electron configuration using a 500-fsec laser pulse. The initial $4p_{3/2}nd$ doubly excited state is energy degenerate with the $4p_{1/2}n'd$ states and several continuum channels. Because of the short-pulse excitation, the initial state of the atom is not an energy eigenstate, but a nonstationary wave packet. As a result, oscillations between the two bound configurations were produced. These oscillations were measured by scanning the timing of a second 500-fsec laser pulse tuned to drive the $4p_{1/2}n'd$ ionic state back down to the $4sn'd$ singly excited configuration, which was subsequently detected using selective field ionization. A simple theoretical model was used to model the experimental results and produced good agreement with the data.

PACS number(s): 32.80.Rm, 33.80.Rv

I. INTRODUCTION

Multichannel quantum defect theory (MQDT) [1–5] with the isolated core excitation (ICE) technique [6–8] have been used extensively and successfully to characterize the complex spectra of many two-electron configurations [9]. In particular, doubly excited states above the first ionization limit played an important role in understanding the electron-electron interaction [10,11]. These doubly excited states are generally produced using ICE, in which one of the ground-state electrons is optically excited to a high Rydberg state, thus isolating the Rydberg electron from the ionic core. After some time, a second photoexcitation promotes the core electron to an excited state, producing a doubly excited state. Above the first ionization limit the eigenstates of the atom are a mixture of a number of bound and unbound configurations. The addition of the continuum configurations results in autoionizing states.

Using a short-pulse laser (shorter than the classical Rydberg orbit period), the system can be prepared to occupy a single bound configuration, resulting in a nonstationary state [12,13]. These states are not energy eigenstates of the atom and thus have a time-dependent probability distribution that can be monitored as the system evolves in time. The transfer of electron population between degenerate bound and continuum configurations is made possible through the Coulomb interaction during collisions between the core electron and the Rydberg electron. The decay of these nonstationary wave packets was successfully modeled in 1991 by Wang and Cooke [14] for the case when a short-pulse laser in conjunction with ICE is used to create these wave packets. A more general MQDT description of the wave packets in two-electron systems has been given by Henle, Ritsch, and Zoller [15].

The optical Ramsey method or bound-state interferometry [16–19] has been used successfully to monitor the decay of these nonstationary wave packets [20]. In this method, two identical short-pulse lasers were used to create two wave packets and the interference signal between these two wave packets was monitored as the timing between the two laser pulses was scanned. From the interference signal it was possible to measure the similarity between the wave packet at time t and the wave packet at $t=0$. A large interference signal corresponds to the two wave packets being very similar, which indicates that the atom is in the same state. As a result the population in the initial state can be probed as a function of time. Recently, two experiments have been performed in which a more direct measurement of the evolution of these wave packets has been made. In the first, a time-of-flight electron detector was used, which showed a nonexponential decay in the autoionization of a shock wave packet [21], and in the second experiment, which used an atomic streak camera [22,23], it was shown that with the application of a static electric field the decay of these wave packets can be altered [24].

In this paper we present a simple and direct measurement of the time evolution of the $4p_{1/2}n'd$ doubly excited states in calcium. The measurement shows an oscillatory behavior between the energy-degenerate $4p_{3/2}nd$ and $4p_{1/2}n'd$ doubly excited channels for the case when the atom at $t=0$ was prepared in a pure $4p_{3/2}nd$ state. To our knowledge this is the first *direct* measurement of this oscillation. In addition, our data suggest that in this energy range autoionization occurs primarily while the wave packet is occupying the $4p_{3/2}nd$ channel. A simple theoretical model is presented that shows a rather good agreement with the experimental results.

II. EXPERIMENTAL PROCEDURE

As shown in Fig. 1, nsec dye laser pulses were used to promote the ground state of calcium to the $4s19d$ Rydberg state. About 50 nsec later the Rydberg atoms were exposed to a 393.5-nm, 500-fsec laser pulse tuned to excite the $4s19d$-$4p_{3/2}19d$ transition. This state is energy degenerate with the $4p_{1/2}n'd$ doubly excited states and with several continuum channels. The excitation with the short laser pulse produced a nearly pure $4p_{3/2}19d$ state, since the excitation time was shorter than the autoionization lifetime of this state.

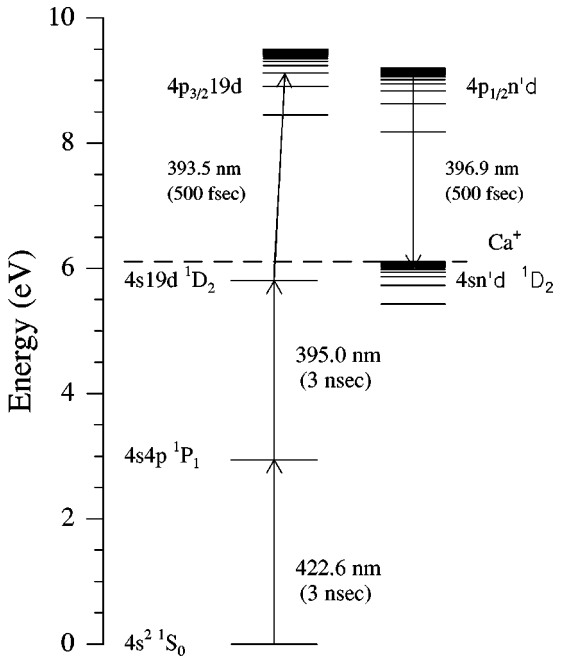

FIG. 1. Excitation diagram for calcium used in the experiment. The first nsec dye laser pulse excites the $4s^2\,S_0$ ground state to a high Rydberg level ($4s19d\ ^1D_2$). About 50 nsec later a 500-fsec short-pulse laser promotes the atom to a pure $4p_{3/2}19d$ doubly excited state. A second 500-fsec short-pulse laser is then used to drive the transition from the $4p_{1/2}n'd$ states to the $4sn'd$ states.

As a result a nonstationary two-electron wave packet was produced. After the laser excitation, the wave packet evolved into degenerate bound and continuum dielectronic configurations. This evolution was monitored by using a second 397-nm, 500-fsec laser pulse, tuned to stimulate the atoms from the $4p_{1/2}n'd$ doubly excited state back down to the $4sn'd$ singly excited neutral configuration. The resulting $4sn'd$ states live for several microseconds, which allowed a selective field ionization detection of these states to be performed. A direct and complete monitoring of the evolution of these autoionizing states was made possible by simply changing the timing between the first and second short-pulse lasers.

The short laser pulses were produced using an amplified self-mode-locked Ti:sapphire laser. The system produced about 4-mJ, 100-fsec laser pulses with a repetition rate of 20 Hz. The full width at half maximum of the amplified short-pulse laser was about 10 nm, with central wavelength at 790 nm. With this much spectral width, it was possible to produce both the core laser wavelengths from a single laser beam simply by splitting the beam into two parts and using two separate 1.2-cm potassium dihydrogen phosphate (KDP) doubling crystals, with each tuned to the proper core laser wavelength. By doing so, we were assured of nearly zero temporal jitter between the two short pulses. Each of the laser beams had a variable optical path length which allowed continuous scanning of the delay between the two laser pulses. The KDP doubling crystals limited the pulse bandwidth to about 30 cm^{-1}, which corresponds to approximately 500-fsec laser pulse duration.

The experiment was performed in a vacuum chamber with background pressures in the low 10^{-7} Torr. All the lasers entered the chamber from a window on the side and interacted with the calcium atomic beam at a right angle. The atomic beam was produced by a resistively heated effusive stainless steel oven that produced an atomic density of about 10^9 atoms/cm^3. Capacitor plates were placed above and below the interaction region with a screen mesh in the top capacitor plate, which allowed electrons to pass. Above the interaction region a pair of microchannel plate charged-particle detectors were used to monitor the electrons produced in the experiment. Detection of the final $4sn'd$ electron population was accomplished using a ramped negative voltage applied on the lower capacitor plate. The ramped voltage was applied at about 100 nsec from the firing of the short-pulse laser. The electric field E that is required to field-ionize a state with principal quantum number n can be calculated using $E=1/16n^4$ a.u. For the case when a ramped electric field $E(t)$ was used, the atom was subjected to an increasing electric-field value. As a result, states with larger principal quantum number n will field-ionize earlier in time than states with smaller n values. This technique allowed the measurement of the population distribution in the final n states to be made.

The experiment consisted of tuning the Rydberg laser to different initial Rydberg states ($n=18$, 19, and 20). In each case the population in the $4p_{1/2}n'd$ doubly excited state was measured as the timing between the two short-pulse lasers was scanned.

III. THEORY

To probe the evolution of these doubly excited states, let us consider first the case when a series of N noninteracting Rydberg states $|\phi_i\rangle$ interact with a bound ''perturber'' state $|\phi_p\rangle$. The eigenstate of the system at a given energy (E_j) becomes a superposition of the Rydberg states and the perturber state,

$$|\psi(E_j)\rangle = C_p(E_j)|\phi_p\rangle + \sum_{i=1}^{N} C_i(E_j)|\phi_i\rangle, \qquad (1)$$

where $C_p(E_j)$ and $C_i(E_j)$ are energy-dependent coefficients that reflect the amounts of the perturber and Rydberg states, respectively, in the eigenstate $|\psi(E_j)\rangle$. In other words, each eigenstate contains a certain amount of perturber character; the largest amount will be in the eigenstates with energies close to the uncoupled perturber's energy. A simple diagonalization exercise shows that the distribution of perturber character among the eigenstates has a Lorentzian line shape. The width of the Lorentzian is a measure of the coupling between the Rydberg states and the perturber state. If a short-pulse laser (with a spectral width larger than the Lorentzian width of the perturber character) has coupling only to the perturber state, then only the eigenstates that have perturber character will be excited; as a result the excited state will be the sum of all these eigenstates,

$$\Psi(t)=\sum_{j=1}^{N} C_p(E_j)\exp(-iE_jt)|\psi(E_j)\rangle. \quad (2)$$

Here $C_p(E_j)$ is the perturber character in the jth eigenstate, which is given by

$$|C_p(E_j)|^2\propto \frac{1}{2\pi}\frac{\Delta E}{(E_j-E_p)^2+(\Delta E/2)^2}. \quad (3)$$

E_j and E_p are the binding energies of the jth eigenstate and the uncoupled perturber state, respectively. ΔE is the width of the Lorentzian distribution of the perturber character.

The wave function in Eq. (2) is not an energy eigenstate of the atom, but a nonstationary wave packet. The evolution of this wave packet can be monitored by calculating the population in the initial state (perturber state) as a function of time. This is simply done by projecting the initial state onto the wave packet in Eq. (2), and thus the probability of being in the initial state is

$$P(t)=|\langle\Psi(t=0)|\Psi(t)\rangle|^2=\left|\sum_{j=1}^{N}|C_p(E_j)|^2\exp(-iE_jt)\right|^2. \quad (4)$$

Comparing this result to the experiment, the perturber state can be considered to be the $4p_{3/2}19d$ ionic state, and the Rydberg states are the $4p_{1/2}n'd$ doubly excited states with $n'\cong 29-33$. In addition to these two bound configurations we also have continuum channels. The inclusion of the continuum channels will result in autoionization. Due to the wave-packet nature of these doubly excited states, the autoionization is not a simple exponential decay [21], as in the case of a long laser pulse.

After the short-pulse excitation, the population in the initial $4p_{3/2}19d$ state will evolve into several other bound and continuum states. The population that evolves into the continuum will be lost (autoionization), but the population that goes into the bound states ($4p_{1/2}n'd$) will survive. Some of this population can then evolve back into the original state, and as a result an oscillatory configuration is produced.

This oscillation can be monitored by measuring the population in either the $4p_{3/2}19d$ or the $4p_{1/2}n'd$ doubly excited states as a function of time. In the experiment presented here the population in the $4p_{1/2}n'd$ states was measured using a second short laser pulse tuned to drive the core electron from the $4p_{1/2}$ to the $4s$ state, thus producing a singly excited stable atom. The population in the $4p_{1/2}n'd$ doubly excited states can be calculated using Eq. (4) (not including autoionization),

$$P_{4p_{1/2}n'd}(t)=[1-P_{4p_{3/2}19d}(t)]. \quad (5)$$

In this model we have made the approximation that autoionization can take place only if the system is in the $4p_{3/2}19d$ state. This assumption was used since the experimental result showed that, while the wave packet occupied the $4p_{1/2}n'd$ states, very little autoionization was recorded. To implement this situation a simple computer program has been developed to calculate the population in the $4p_{1/2}n'd$ states as a function of time. In each time step the program calculates the population in Eq. (5) and multiplies it by an autoionization factor that depends only on the population in the $4p_{3/2}19d$ state and the rate at which this state will autoionize. As a result a complete and accurate measurement of the final population was accomplished.

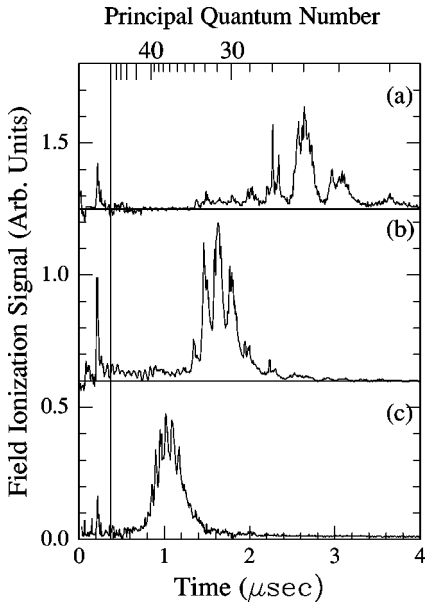

FIG. 2. The field-ionization signal of the final $4sn'd$ states is shown. In (a)–(c) the Rydberg laser tuning was chosen to populate one of three possible Rydberg states, $n=18$, 19, and 20, respectively. The large signal at about 200 nsec represents the autoionization signal. The ramped electric field was applied ~200 nsec after the short-pulse laser was fired and had a rise time of 4 μsec, which produced the time-resolved Rydberg signal seen in (a)–(c). The beginning of the ramp is marked on the figure by the solid vertical line. The signal in (a)–(c) represents the population that evolved into the $4p_{1/2}n'd$ states from the initial $4p_{3/2}nd$ state at a given time. The data in (a) were for the case when $n=18$; the evolution was primarily to three n' states centered at $n'=27$. In (b) the initial state was $n=19$, and evolution was to about five states centered at $n'=31$. For the case in (c) the initial state was $n=20$ and the evolution was to about nine states centered at $n'=38$.

IV. RESULTS AND DISCUSSIONS

Figures 2(a)–2(c) show a field-ionization signal of the final $4sn'd$ states for three different initial Rydberg states, $n=18$, 19, and 20, respectively. The signal represents the population distribution in the $4p_{1/2}n'd$ doubly excited states. This measurement was achieved by tuning the second short-pulse laser to drive the $4p_{1/2}n'd$-$4sn'd$ transition, thus stabilizing the atom into the bound singly excited state. During this transition the Rydberg electron population distribution remained unperturbed since the laser was tuned directly on the ionic resonance [11]. The final $4sn'd$-state population was measured using selective field ionization.

Figure 3 represents the population in the $4p_{1/2}n'd$ doubly excited state as the timing between the two short-pulse lasers was changed. At $t=0$ the wave packet is in a pure $4p_{3/2}19d$

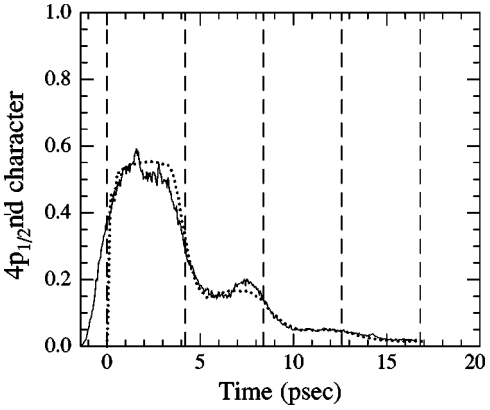

FIG. 3. The population in the $4p_{1/2}n'd$ states as a function of time is shown for the case when the initial state of the atom was the $4p_{3/2}19d$ state. The solid line represents our experimental data. The dotted line is our theoretical calculation and the vertical dashed lines are the classical Kepler orbit periods of the $4p_{1/2}n'd$ Rydberg electron.

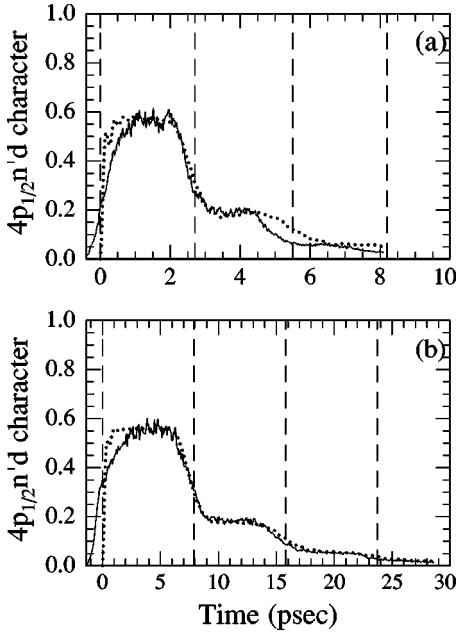

FIG. 4. The population in the $4p_{1/2}n'd$ states as a function of time for two different initial Rydberg states is shown. The data in (a) were for the case when the initial state of the atom is $4p_{3/2}18d$, and the data in (b) were for the case when the initial state of the atom was $4p_{3/2}20d$. The solid lines represent our experimental data. The dotted lines are our theoretical calculations and the vertical dashed lines are the classical Kepler orbit periods of the $4p_{1/2}n'd$ Rydberg electron.

state. However, the interaction between the two electrons rapidly spreads the character among the other bound and continuum channels. For this case, approximately 60% of the population evolved into the $4p_{1/2}n'd$ states, with $n' \cong 29-33$. Since the Rydberg states that make up the wave packet in this case have a much longer Kepler period than the initial $n=19$ state, the evolution of the wave packet in these states is expected to take much longer, and thus the atom will spend a longer time in the $4p_{1/2}n'd$ channel. This behavior can be observed in the relatively flat regions in Fig. 3. These flat regions also suggests that very few autoionization events take place while the wave packet occupies the $4p_{1/2}n'd$ states.

Upon the first return of the wave packet to the core (marked by the dashed vertical lines in Fig. 3), additional scattering events take place. As a result, some population will evolve back into the bound $4p_{3/2}19d$ state and some will transfer to the continuum. The population that scatters into the $4p_{3/2}19d$ state will evolve very quickly, since the Kepler period of this state is much shorter (<1 psec). During this time the atoms go through a period of rapid autoionization in which a great deal of the population is lost; in our data about 20% of the population returns to the $4p_{1/2}n'd$ states. This return of the population to the $4p_{1/2}n'd$ states is clearly shown by the increase in the population after the first oscillation. A second oscillation can also be observed where about 5% of the population survives. This oscillation is less pronounced since most of the population is already lost through autoionization.

The dotted line in Fig. 3 represents our theoretical calculation of the population in the $4p_{1/2}n'd$ states as a function of time using Eq. (5). The calculation shows very good agreement with the experimental results. The deviation from the experimental data at very short times is due to the fact that this model is based on the assumption that the initial state of the atom (at $t=0$) is a pure $4p_{3/2}19d$ state. This condition can be produced if a very short laser pulse is used to excite the core electron. In our experiment the exciting laser had a width of approximately 500 fsec, which was sufficiently short to produce a nearly pure $4p_{3/2}19d$ initial state. The theoretical calculation was done using Eq. (5), where in each time step the computer program calculated the population in Eq. (5) and multiplied it by an autoionization factor that depended only on the population in the $4p_{3/2}19d$ state and the rate at which this state autoionized. This autoionization rate was the only fitting parameter in this model. The rate that was used to fit the experimental result in Fig. 3 was 4.1×10^{-5} a.u. This rate is in reasonable agreement with the value of 5.6×10^{-5} a.u. reported by Jones in Ref. [25].

Figures 4(a) and 4(b) represent the population in the $4p_{1/2}n'd$ states for two different initial Rydberg states, $n=18$ and 20, respectively. For the case when $n=20$, the initial wave packet scatters into about seven $4p_{1/2}n'd$ states centered about $n'=38$, and for the case when $n=18$, the wave packet scatters to only three $4p_{1/2}n'd$ states centered at $n'=27$. The Kepler period of the Rydberg state is almost invariant when the atom is occupying the different $4p_{3/2}nd$ states, but as the wave packet scatters into the $4p_{1/2}n'd$ states, the Kepler period of the Rydberg states changes dramatically. This effect is clearly shown in the data in Figs. 4(a) and 4(b) where the oscillation period is about three times longer in the case when the initial state is in $n=20$. The dotted lines in Fig. 4 are the calculation using our simple model that we described earlier. The autoionization rate parameters that were used to fit the data in Figs. 4(a) and 4(b) are 5.9×10^{-5} and 3.9×10^{-5} a.u., respectively. The rates from Ref. [25] are 7×10^{-5} and 5.7×10^{-5} a.u., respectively,

which still show good agreement. It is also noted that the deviation of our theoretical model from the experimental data is largest in Fig. 4(a). This is due to the fact that the 500-fsec exciting laser pulse width was short enough to produce nearly pure initial states in the cases of $n=19$ and 20, but not short enough to produce the same initial-state purity in the case of $n=18$. As a result, a slight different oscillation pattern is expected to be produced in the experiment.

V. CONCLUSIONS

In this paper we have demonstrated a simple and direct measurement of the oscillation between degenerate bound states in a rapidly autoionizing energy configuration. To the best of our knowledge this is the first direct measurement of this oscillation. In addition to that, our data show that during the time the wave packet is in the $4p_{1/2}n'd$ bound states the atoms have very few autoionization events. This is primarily due to the long Kepler period of these Rydberg states. Finally, a simple time-dependent theoretical model has been described which shows rather good agreement with our experimental results.

ACKNOWLEDGMENTS

The authors would like to thank Robert R. Jones from the University of Virginia for the numerous helpful discussions about setting up the short-pulse-laser system. This work was supported by the National Science Foundation (Grant No. 9722561) and by the University of Missouri Research Board.

[1] U. Fano, Phys. Rev. A **2**, 353 (1970).
[2] A. Guisti-Suzor and U. Fano, J. Phys. B **17**, 215 (1984).
[3] W. E. Cooke and C. L. Cromer, Phys. Rev. A **32**, 2725 (1985).
[4] C. H. Greene and M. Aymar, Phys. Rev. A **44**, 1773 (1991), and references therein.
[5] R. R. Jones, C. J. Dai, and T. F. Gallagher, Phys. Rev. A **41**, 316 (1990).
[6] T. F. Gallagher, J. Opt. Soc. Am. B **4**, 794 (1987), and references therein.
[7] W. Sandner, Comments At. Mol. Phys. **20**, 171 (1987), and references therein.
[8] W. E. Cooke, T. F. Gallagher, S. A. Edelstein, and R. M. Hill, Phys. Rev. Lett. **40**, 178 (1978).
[9] T. F. Gallagher, *Rydberg Atoms*, 1st ed. (Cambridge University Press, Cambridge, England, 1994).
[10] J. G. Story, D. I. Duncan, and T. F. Gallagher, Phys. Rev. Lett. **71**, 3431 (1993).
[11] Heider N. Ereifej and J. G. Story, Phys. Rev. A **60**, 3947 (1999).
[12] D. W. Schumacher, D. I. Duncan, R. R. Jones, and T. F. Gallagher, J. Phys. B **29**, L1 (1996).
[13] D. W. Schumacher, B. J. Lyons, and T. F. Gallagher, Phys. Rev. Lett. **78**, 4359 (1997); B. J. Lyons, D. W. Schumacher, D. I. Duncan, R. R. Jones, and T. F. Gallagher, Phys. Rev. A **57**, 3712 (1998).
[14] X. Wang and W. E. Cooke, Phys. Rev. Lett. **67**, 976 (1991).
[15] W. A. Henle, H. Ritsch, and P. Zoller, Phys. Rev. A **36**, 683 (1987).
[16] N. F. Scherer *et al.*, J. Chem. Phys. **93**, 856 (1990).
[17] L. D. Noordam, D. I. Duncan, and T. F. Gallagher, Phys. Rev. A **45**, 4734 (1992).
[18] B. Broers, J. F. Christian, J. H. Hoogenraad, W. J. van der Zande, H. B. van Linden van den Heuvell, and L. D. Noordam, Phys. Rev. Lett. **71**, 344 (1993).
[19] R. R. Jones, C. S. Raman, D. W. Schumacher, and P. H. Bucksbaum, Phys. Rev. Lett. **71**, 2575 (1993).
[20] M. B. Campbell, T. J. Bensky, and R. R. Jones, Phys. Rev. A **57**, 4616 (1998).
[21] J. E. Thoma and R. R. Jones, Phys. Rev. Lett. **83**, 516 (1999).
[22] G. M. Lankhuijzen and L. D. Noordam, Opt. Commun. **129**, 361 (1996).
[23] G. M. Lankhuijzen and L. D. Noordam, Phys. Rev. Lett. **76**, 1784 (1996).
[24] J. B. M. Warntjes, C. Wesdorp, F. Robicheaux, and L. D. Noordam, Phys. Rev. Lett. **83**, 512 (1999).
[25] R. R. Jones, Phys. Rev. A **58**, 2608 (1998).